Physics – Uspekhi **55** (12) 1255 – 1267 (2012)

CONFERENCES AND SYMPOSIA PACS numbers: 01.10.Fv, **61.72.–y**, **62.20.–x**, **62.30.+d**, **75.47.–m**, **75.75.–c**, **85.75.–d**

Spintronics and nanomagnetism
(Scientific session of the Physical Sciences Division of the Russian Academy of Sciences, 25 April 2012)

DOI: 10.3367/UFNe.0182.201212g.1345

A scientific session of the Physical Sciences Division of the Russian Academy of Sciences (RAS), entitled "Spintronics and nanomagnetism", was held on 25 April 2012 at the conference hall of the Lebedev Physical Institute, RAS.

The agenda of the session announced on the RAS Physical Sciences Division website www.gpad.ac.ru included the following reports:

(1) **Zvezdin A K, Zvezdin K A** (Prokhorov General Physics Institute, Russian Academy of Sciences, Moscow), **Popkov A F** (National Research University 'Moscow State Institute of Electronic Technology', Moscow) "Spin moment transfer effects and their applications in spintronics";

(2) **Fraerman A A** (Institute for Physics of Microstructures, Russian Academy of Sciences, Nizhny Novgorod) "Magnetic states and transport properties of ferromagnetic nanostructures";

(3) **Panin V E, Egorushkin V E, Panin A V** (Institute of Strength Physics and Materials Science, Siberian Branch of the Russian Academy of Sciences, Tomsk) "Nonlinear wave processes in a deformable solid as in a multiscale hierarchically organized system".

Papers based on oral reports 2 and 3 are presented below.

PACS numbers: **75.47.–m**, **75.75.–c**, **85.75.–d**
DOI: 10.3367/UFNe.0182.201212h.1345

Magnetic states and transport properties of ferromagnetic nanostructures

A A Fraerman

1. Introduction

There are at least two motivating factors for research interests in the transport properties of ferromagnetic nanostructures. First, conducting ferromagnets, which are the ones to be discussed below, have their current carriers spin-polarized. Their energy spectra are split into two subbands, in one of which the occupying electrons align their spin projections parallel and, in the other, antiparallel to the magnetic moment of the sample. The spin 'splitting' compares to the Curie temperature of these materials to an order of magnitude. It may be considered that in ferromagnets there is a colossal 'exchange' field of strength $H \sim k_B T_c/\mu_B \sim 10^6 - 10^7$ Oe (k_B is the Boltzmann constant, and μ_B is the Bohr magneton). Prior to the discovery of giant magnetoresistance [1–2] (see also Ref. [3] on the tunneling version of the effect), such an 'exchange' field had not manifested itself in the transport and optical properties of ferromagnets, which were determined by the relatively weak spin-orbit interaction [4] rather than the Coulomb interaction. This discovery has greatly stimulated renewed efforts to study spin-dependent transport effects.

Second, nanostructure formation methods, which have been the subject of intense development in recent years, are an effective tool for controling the magnetic state of a ferromagnet. It is known [5] that the magnetization distribution in a ferromagnetic sample is determined by competition among the magnetic anisotropy, the exchange interaction, and the magnetostatic interaction. The magnetic domain structure that results from this competition is not universal, but rather depends on the sample shape and dimensions. Nanostructure patterning allows one to control these parameters and, hence, magnetization distribution in the most important nanometer range. As far as this range is concerned, the important special feature of ferromagnets is the presence in them of two characteristic scales: the domain wall thickness and the exchange length, both measuring tens of nanometers for transition metal ferromagnets.

Thus, the search for new transport and optical effects of an 'exchange' nature in ferromagnetic nanostructures constitutes a topical and exciting task. This report briefly reviews the relevant research that has been done at the Institute for Physics of Microstructures, RAS.

2. 'Exchange' versions of the Hall and diode effects

Let us start by examining phenomenologically the possibility of transport effects of an exchange nature in inhomogeneous ferromagnets.

In a conducting medium under the influence of a constant electric field **E**, an electric current density **j** arises in the following form

$$j_i = \sigma_{ik} E_k + \gamma_{ijk} E_j E_k + \ldots \quad (1)$$

where the linear and quadratic conductivity tensors depend on the sample's magnetic moment and its spatial derivatives.

A A Fraerman Institute for Physics of Microstructures, Russian Academy of Sciences, Nizhny Novgorod, Russian Federation
E-mail: andr@ipm.sci-nnov.ru

Uspekhi Fizicheskikh Nauk **182** (12) 1345 – 1357 (2012)
DOI: 10.3367/UFNr.0182.201212g.1345
Translated by E G Strel'chenko, S N Gorin; edited by A Radzig

Uspekhi Fizicheskikh Nauk **182** (12) 1345 – 1351 (2012)
DOI: 10.3367/UFNr.0182.201212h.1345
Translated by E G Strel'chenko; edited by A Radzig

The problem that faces us consists in determining these dependences. Restricting the discussion to nondissipative processes in media with a center of inversion, we conclude that the linear and nonlinear conductivity tensors contain terms of odd powers in the magnetic moment $\mathbf{M}$, with the σ_{ik} and γ_{ijk} tensors having terms with even and odd powers of spatial derivatives, respectively. Assuming the exchange interaction to be responsible for the effects we are looking for, let us require that the expression for the current (1) be invariant under the coherent rotation of the sample's magnetic moment [5, 6]. This means that conductivity tensors must not comprise convolutions of 'spatial' indices with 'magnetic' ones). With all of the above requirements met, the following equation is derived for the electric current flowing in an inhomogeneously magnetized conducting ferromagnet [7, 8]:

$$j_i = \sigma\left(\mathbf{M}\left[\frac{\partial \mathbf{M}}{\partial x_i}\times\frac{\partial \mathbf{M}}{\partial x_k}\right]\right)E_k + \gamma\left(\mathbf{M}\left[\frac{\partial \mathbf{M}}{\partial x_i}\times\frac{\partial^2 \mathbf{M}}{\partial x_j\,\partial x_k}\right]\right)E_jE_k + \ldots, \tag{2}$$

where σ, γ are the scalar constants (we confine ourselves to studying media with isotropic or cubic crystalline structures). The linear conductivity tensor, which is antisymmetric, describes the contribution of an exchange nature to the Hall effect, whereas the second term on the right-hand side of equation (2) is responsible for the rectifying properties of the ferromagnet. Both tensors found are nonzero only in those ferromagnets where the magnetic moment vectors do not lie in the same plane, i.e., in samples with noncoplanar magnetization distribution. To see that this is indeed the case, note that expressions for the conductivity tensors can be readily obtained by expanding the mixed product $\mathbf{M}_1[\mathbf{M}_2\times\mathbf{M}_3]$ in a Taylor series, where $\mathbf{M}_{1,2,3}$ are the magnetic moments at the neighboring points in the sample. If the linear conductivity tensor is different from zero in systems with a nononedimensional distribution of the magnetic moment, it follows that a sample with a one-dimensional noncoplanar magnetization distribution should also have rectifying properties.

Two examples of noncoplanar magnetic moment distribution are worth considering. Suppose a ferromagnet has a magnetization distribution of the form

$$\mathbf{M} = \big(\sin\theta(\rho)\,\cos(\nu\varphi+\varphi_0),\ \sin\theta(\rho)\sin(\nu\varphi+\varphi_0),\ \cos\theta(\rho)\big), \tag{3}$$

where φ, ρ are cylindrical coordinates, ν is an integer, and φ_0 is a (constant) phase shift. Substituting Eqn (3) into expression (2) yields

$$\mathbf{j} = \mathbf{E}\times\mathbf{B}_{\text{eff}}\,,\qquad B_{\text{eff}} = \sigma\left(\mathbf{M}\left[\frac{\partial \mathbf{M}}{\partial x}\times\frac{\partial \mathbf{M}}{\partial y}\right]\right) = \sigma\nu\,\frac{1}{\rho}\,\frac{\partial\cos\theta}{\partial\rho}\,, \tag{4}$$

implying that a vortex ($\nu = 1$, $\varphi_0 = \pm\pi/2$) or an antivortex ($\nu = -1$, $\varphi_0 = 0, \pi$) noncoplanar magnetic moment distribution can be expected to provide an additional contribution to the Hall effect. For a distribution in the form of a conical magnetic spiral, namely

$$\mathbf{M}(z) = \big(m\cos(qz)\,,\ m\sin(qz)\,,\ m_z\big)\,,\qquad \mathbf{M}^2 = m^2 + m_z^2\,, \tag{5}$$

the result of such a substitution reduces to

$$j_z = \gamma q^3 m_z(1-m_z^2)\,E_z^2\,, \tag{6}$$

suggesting the existence of diode properties in such a structure. A classical model proposed in Ref. [9] deduces the 'exchange' contribution to the Hall conductivity from the noncollinearity between the magnetic moment of a moving particle and the external field and can be used as a basis to explain, at least in part, the microscopic mechanism of the effects being discussed.

3. Optical and neutron-optical effects

To describe conduction electrons in ferromagnets, the simplest quantum-mechanical approach is to apply the Vonsovskii–Zener s-d model, in which the problem reduces to that of finding the eigenfunctions and eigenvalues of the Schrödinger equation

$$-\Delta\Psi(\mathbf{r}) - J\mathbf{M}(\mathbf{r})\,\hat{\boldsymbol{\sigma}}\,\Psi(\mathbf{r}) = E\Psi(\mathbf{r})\,, \tag{7}$$

where $\hat{\boldsymbol{\sigma}}$ is the Pauli matrix vector, J is the exchange interaction constant between the conduction s and localized d electrons, and $\mathbf{M}$ is the unit vector in the direction of the magnetic moment. Note the analogy between the s-d model description of conduction electrons in ferromagnets and the description of neutrons for which the magnetic moment vector in equation (7) should be replaced by the magnetic induction vector $\mathbf{B}$, and the exchange constant by the Bohr nuclear magneton [10]. This analogy provides a common framework for discussing the transport and optical properties of conducting ferromagnets, on the one hand, and neutron scattering by inhomogeneous magnetic systems, on the other hand.

For the case of a magnetic spiral defined by formula (5), equation (7) can be solved exactly [11] to yield the following expressions for the spectrum and eigenfunctions of the system:

$$E_\pm = k^2 + p^2 + \left(\frac{q}{2}\right)^2 \pm \sqrt{q^2k^2 + J^2 - 2m_zJqk}\,, \tag{8}$$

$$\Psi_\pm = \frac{1}{\sqrt{1+\delta_\pm(k)}}\begin{pmatrix}\delta_\pm(k)\exp\left(-\dfrac{\mathrm{i}qz}{2}\right)\\ \exp\left(\dfrac{\mathrm{i}qz}{2}\right)\end{pmatrix}\exp(\mathrm{i}kz)\exp(\mathrm{i}\mathbf{p}\boldsymbol{\rho})\,,$$

$$\delta_\pm = \frac{m_zJ - qk \pm \sqrt{q^2k^2 + J^2 - 2m_zJqk}}{J(1-m_z^2)^{1/2}}\,, \tag{9}$$

where k, $\mathbf{p}$ are the electron quasimomenta along and perpendicular to the spiral axis, respectively.

From expression (8) it follows that the spectrum of current carriers in a conical ($m_z \neq 0$) spiral is not an even function of quasimomentum. Thus, the electrons moving to the left along the spiral axis have different group velocities from those moving to the right. In a macroscopic system, this difference does not produce an electric current because it is exactly compensated for by the difference in the number of opposite-moving equilibrium electrons. In mesoscopic systems, however — such as small ferromagnetic rings with a noncoplanar distribution of the magnetic moment — the removal of Kramers degeneracy and the quantization of quasimomentum can lead to the appearance of predicted [12, 13] persistent electric currents.

In a conical magnetic spiral, spectral asymmetry is responsible for the occurrence of the diode effect, with 'easy' current flow direction being determined by the sign of the spiral wave number (left–right spiral) and by where the perpendicular magnetic moment component m_z is directed [see formula (6)]. The important point is that, as can be seen from Eqn (9), the wave function components — and hence the expectation value of the electron's intrinsic magnetic moment — depend on the quasimomentum component along the spiral axis. This results, in particular, in electron scattering by nonmagnetic impurities becoming asymmetric, thus adding to the diode effect [7]. Similar effects (asymmetry in both the group velocity and the scattering rate by nonmagnetic impurities) are responsible for the peculiarities in the spatial dispersion of the dielectric constant. For a conical magnetic spiral, the expansion of the dielectric constant may contain an additional term of the form [14]

$$\varepsilon_{ii} = K_{ii}\left(\mathbf{M}\left[\frac{\partial \mathbf{M}}{\partial z} \times \frac{\partial^2 \mathbf{M}}{\partial z^2}\right]\right) k_z\,, \tag{10}$$

where k_z is the spiral axis component of the electromagnetic wave vector.

Of special note is that the electric component of an electromagnetic wave can induce transitions between spin subbands in noncollinear and noncoplanar magnetic systems. Using the wave functions of Eqn (9), the probability of electric dipole transitions between spin subbands in a magnetic spiral is readily found to be [15]

$$W^{\pm}_{k,k'} = \frac{2\pi}{\hbar}\left(\frac{JeE_z q}{2m\omega^2}\right)^2 (1 - m_z^2)\,\delta(\mathbf{k} - \mathbf{k}')\,\delta\big(\Delta E\,(k_z) - \hbar\omega\big), \tag{11}$$

where ω is the electromagnetic wave frequency, ΔE is the energy spacing between the spin subbands, and $\delta(x)$ is the delta function. In noncollinear systems, these transitions make an additional contribution to radiation absorption, as analyzed in detail in paper [16]. In a noncoplanar magnetic system (such as a conical magnetic spiral), the electric dipole transitions (11) give rise to a constant electric current, i.e., to the photogalvanic effect [15].

Let us consider some features of neutron scattering by noncoplanar magnetic systems. It is known [10] that the interaction between cold neutrons and a magnetic field is sufficiently weak for the scattering cross section to be representable as a power series in the magnetic induction $\mathbf{B}$. The only factor determining the interaction between a magnetic field and a neutron spin is the angle between them. Hence, the total scattering cross section (summed over the spin polarizations of the incident and scattered neurons) should be invariant with respect to coherent rotation of the magnetic field at any point in space. Given the above, the scattering cross section can be expressed as

$$\begin{aligned}\sigma\big(\mathbf{k}, \mathbf{k}', \mathbf{B}(\mathbf{r})\big) &= \sigma_0(\mathbf{k}, \mathbf{k}') \\ &+ \int Q_1(\mathbf{k}, \mathbf{k}'; \mathbf{r}_1, \mathbf{r}_2)\big(\mathbf{B}(\mathbf{r}_1)\,\mathbf{B}(\mathbf{r}_2)\big)\,\mathrm{d}\mathbf{r}_1\,\mathrm{d}\mathbf{r}_2 \\ &+ \int Q_2(\mathbf{k}, \mathbf{k}'; \mathbf{r}_1, \mathbf{r}_2, \mathbf{r}_3)\big(\mathbf{B}(\mathbf{r}_1)\big[\mathbf{B}(\mathbf{r}_2) \times \mathbf{B}(\mathbf{r}_3)\big]\big)\,\mathrm{d}\mathbf{r}_1\,\mathrm{d}\mathbf{r}_2\,\mathrm{d}\mathbf{r}_3 + \ldots,\end{aligned} \tag{12}$$

where $\mathbf{k}$, $\mathbf{k}'$ are the incident and scattered neutron wave vectors, and $Q_{1,2}$ are the scalar functions. Because the scattering cross section should obey the reciprocity theorem $\sigma\big(\mathbf{k}, \mathbf{k}', \{\mathbf{B}(\mathbf{r})\}\big) = \sigma\big(-\mathbf{k}', -\mathbf{k}, \{-\mathbf{B}(\mathbf{r})\}\big)$, it follows that the last term in Eqn (12) describes the 'nonreciprocal' contribution, due to the noncoplanar nature of the magnetic induction distribution. Note that calculating this contribution requires going beyond the Born approximation commonly used in the calculation of the cold neutron scattering cross section. See Refs [17, 18] for a discussion of how the nonreciprocal features in the scattering of neutrons manifest themselves in noncoplanar magnetic structures.

Thus, based on the theoretical discussion above, a whole series of new and interesting effects — transport, optical and neutron-optical — are likely to occur in ferromagnetic nanostructures with a noncoplanar, specifically, vortex and spiral, magnetization distribution. Sections 4 and 5 describe methods for creating and experimentally investigating ferromagnetic nanostructures with chirally distributed magnetization.

4. Ferromagnetic nanostructures with vortex distribution of magnetization

The vortex distribution of magnetization [$\nu = 1$, $\varphi_0 = \pm\pi/2$ in formula (3)] is the ground state of a ferromagnetic disc, provided that the radius and height of the disc are larger than the exchange length $l_{\mathrm{ex}} \approx \sqrt{J/M_s^2} \sim 20$ nm [19]. The techniques we used to create such particles involved magnetron sputtering and electronic lithography (Supra 50 V microscope with a lithographical attachment ELPHY Plus) [8, 20, 21]. To effectively control the magnetic state of a nanostructured sample requires that both the geometric dimensions of the sample and its crystalline structure be controlled. For our purposes, polycrystalline samples with a crystallite size of ≈ 20 nm and a sufficiently low ($\approx 20-30$ Oe) coercive force are suitable. Magnetization curves of ferromagnetic films were measured magnetooptically before the lithography process began. The magnetic states of the particles were investigated by magnetic-force microscopy (Solver-HV vacuum probe microscope). The details of the probe measurements performed are presented in Refs [8, 20–22]. Using this method, the vortex state in elliptic ferromagnetic particles was studied in detail, as was the possibility of utilizing the magnetic tip of a probe microscope to control these states.

In symmetrically shaped particles, the magnetic vortex state is degenerate with respect to the vorticity direction, making the particles with left- and right-rotating vortices ($\varphi_0 = \pm\pi/2$) equal in number [23]. For asymmetrical (for example, triangular) particles (see Fig. 1a), if the magnetic field is applied along the triangle bases, it takes different field strengths to produce 'left' and 'right' vortices [24], thus allowing for a lattice of particles with the same sign of vorticity to be created. Shown in Fig. 1b is a magnetic-force image of the remanent state of a lattice of triangular particles. It is seen that all the particles have the same sign of vorticity which can be controlled by changing the direction of the demagnetizing magnetic field. What makes this system remarkable is the presence of a macroscopic toroidal magnetic moment $\mathbf{T} = (1/N)\sum_i [\mathbf{r}_i \times \mathbf{M}_i] \neq 0$, a fact which should, in turn, lead to nonreciprocality in light diffraction by such a lattice. Our recent experiments [25] completely confirmed this prediction.

It seems of interest to fabricate a nanostructure with the antivortex distribution of magnetic moment [$\nu = -1$, $\varphi_0 = 0, \pi$ in formula (3)]. For such a distribution, the Hall voltage reverses sign relative to that in the vortex system [see

formula (4)]. The integer ν is a topological charge of the soliton [26, 27]. The direct proportionality between the Hall voltage and the topological charge of the magnetization distribution justifies naming this effect the 'topological' Hall effect [28]. That the antivortex state is difficult to realize is explained by the presence of excess (relative to the vortex state) magnetostatic energy proportional to the particle volume [8].

Our way to still achieve the goal was to make a lattice of cross-shaped ferromagnetic particles (Fig. 2a) with a feature of increased width on two of the four sides of the cross. The external magnetic field was applied at an angle of 45° to the sides of the cross-shaped particle, as shown by the arrow in Fig. 2a. The remanent states of the system following magnetization in external fields of 1 kOe and 250 Oe are shown in the respective Fig. 2b and 2c, corresponding, respectively, to the quasiuniform magnetic state of the crosses and to the antivortex state of the particles, the latter manifesting itself in that, close to the cross edges, the distribution of 'magnetic charges' changes its symmetry from dipole to quadrupole.

5. Ferromagnetic nanostructures with a spiral magnetization distribution

A noncollinear state can form in a multilayered ferromagnetic nanoparticle due to the magnetostatic interaction between the layers, the stability of the state being determined by the shape of the particle [29].

Let us consider three homogeneous magnetized magnetic discs with dielectric interlayers between them. The magnetostatic interaction between the layers is antiferromagnetic in character, resulting, as shown theoretically [30, 31], in the ground state of the system being spiral (provided that the interaction energy between the discs is much higher than the energy of anisotropy due to, for example, the disc shape). The magnetic state of a multilayered particle can be analyzed experimentally by examining the dependence of its electrical

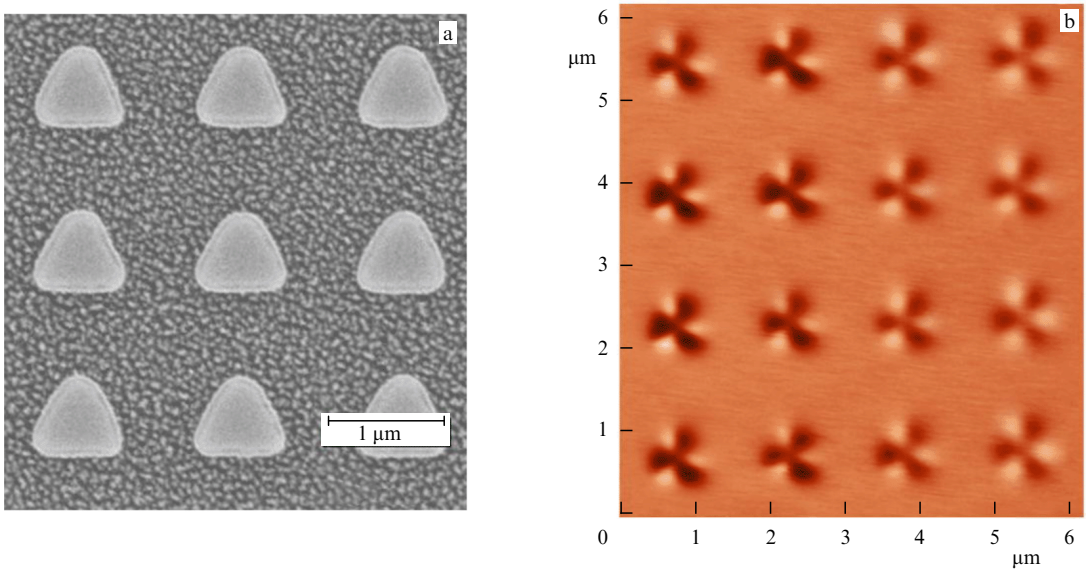

Figure 1. (a) Electron microscopic image of a lattice of triangular particles. (b) Magnetic-force image of the remanent state of this lattice following magnetization in a strong magnetic field applied along the triangle bases.

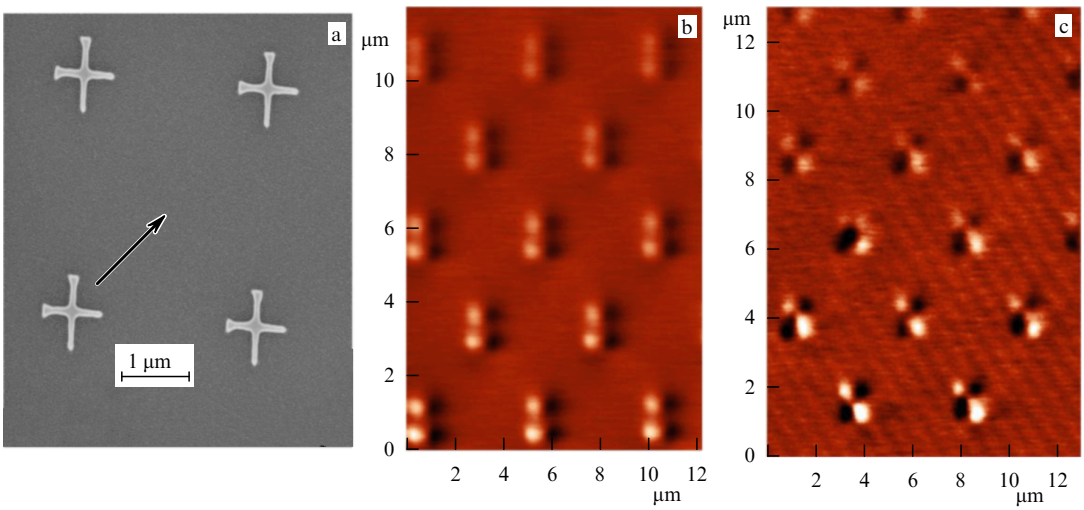

Figure 2. (a) Electron microscopic image of a lattice of cross-shaped particles. (b) Magnetic-force image of the remanent state of this lattice following magnetization in a 1-kOe external field applied in the direction shown by the arrow in Fig. 2a. (c) Magnetic-force image of the remanent state of the lattice of particles following the application of a 250-Oe field.

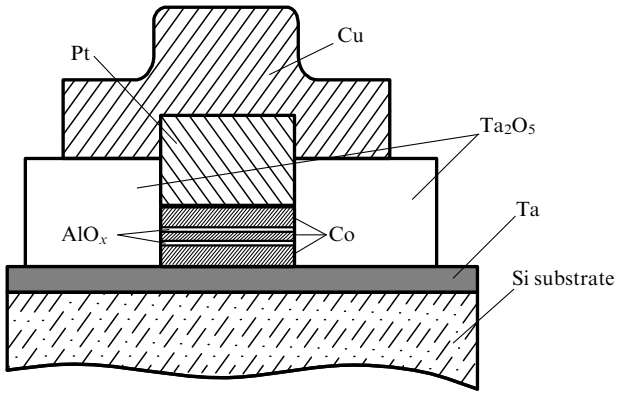

Figure 3. Schematic of a multilayered magnetic particle built into a thin-film electrode system.

resistance on the external magnetic field. Assuming that the field dependence is due to effects of an exchange nature and proportional to the scalar product of the layer magnetic moments [32], we have

$$R = R_{01} + R_{02} - R_1 \cos\theta_{12} - R_2 \cos\theta_{23}\,, \qquad (13)$$

where $\theta_{12}(\theta_{23})$ is the angle between the magnetic moments of the first and second (second and third) discs, R_{01}, R_1 (R_{02}, R_2) is the resistance of the first (second) tunnel junction for the disc magnetic moments oriented parallel, and $\theta_{12} = \theta_{23} = 0$. Alternatively, the magnetic states of multilayered particles can be investigated by magnetic-force microscopy, but the fact that the signal to measure is dominated by the contribution from the upper magnetic layer [30] makes this approach difficult to apply.

Figure 3 depicts a schematic of a multilayered magnetic particle built into a thin-film electrode system connected to a measuring device. The magnetic particle was prepared from a Co(10 nm)/AlO_x(2 nm)/Co(5 nm)/AlO_x(2 nm)/Co(10 nm) thin-film structure. We give elsewhere [29] a detailed description of the preparation method.

Figure 4a shows, for a circular particle ≈ 250 nm in diameter, the measured relative change in resistance, $r(H) = (R(H) - R(H \to \infty))/R(H \to \infty)$, as a function of the externally applied magnetic field (directed as shown by the arrow). The multilayered particle possesses a minimum resistance in large magnetic fields, $|H| > 400$ Oe, and a maximum resistance in low fields, $|H| < 200$ Oe. When the external magnetic fields are large, all the discs have their magnetic moments aligned and, according to formula (13), the resistance of the system is a minimum. As the magnetic field is decreased in magnitude, the layer magnetic moments dissalign, leading to increased resistance.

It is the region of small magnetic fields which is of particular interest. After reaching a maximum, the resistance of the system again decreases, and in a zero field its relative change is $r(0) \approx 0.75\, r_{\max}$, where $r_{\max}$ is the value of r at a maximum. Changing the direction of the external magnetic field results in a dramatic increase in the sample's resistance (segment A–B in Fig. 4a). As the field is increased further, the resistance reaches a maximum again. This resistance versus external magnetic field behavior suggests the layer magnetizations are distributed in a noncollinear fashion in a zero external field.

Suppose that the magnetic moment distribution corresponding to the resistance maximum is collinear 'antiferromagnetic', and that in the absence of a field the symmetric noncollinear state $\theta_{12} = \theta_{23} = \theta$ is realized. Then, using formula (13) and the experimental value $r(0) = 0.75\, r_{\max}$ yields $\theta \approx 120°$. Computer simulation results confirm this scenario.

As the particle anisotropy increases, the angular phases become unstable, resulting in the fact that the resistance versus magnetic field dependence has a number of features that correspond to transitions between collinear phases. The multilayered particles prepared had the same layer thickness as the first sample, but the layer lateral size was taken to be 100×200 nm. The ferromagnetic layers were taken to be CoFe films whose coercivity exceeded that of Co films but which allowed achieving the higher values of $r(H)$.

Figure 4b plots the relative change in the resistance of this sample as a function of the external field strength applied along the long axis of the particle. One does indeed see jumps in resistance which correspond to transitions between the

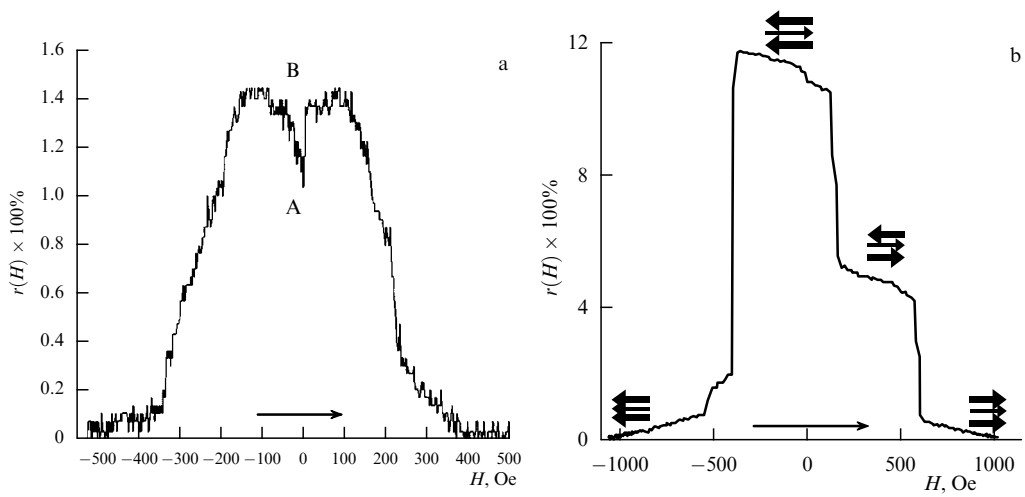

Figure 4. (a) Experimental $r(H)$ data for a circular particle 250 nm in diameter for layer thicknesses Co(10 nm)/AlO_x(2 nm)/Co(5 nm)/ AlO_x(2 nm)/Co(10 nm); the arrow shows the direction of the change in the outer magnetic field. (b) The same for an 'elliptic' particle with lateral dimensions of 200×100 nm for layer thicknesses CoFe(10 nm)/AlO_x(2 nm)/CoFe(5 nm)/AlO_x(2 nm)/ CoFe(10 nm); the magnetic field is directed along the long axis of the particle.

collinear states marked in the figure. Using experimental data, we find that the 'magnetically dependent' parts of transition resistances $R_{1,2}$ (see formula (13)) differ by 20% or less. There are two points to note from the results of this experiment. First, the two tunneling junctions in series that make up the structure under study share a sufficiently high degree of identity. Second, anisotropy plays a fundamental role in the formation of noncollinear states.

6. Conclusion

To summarize, this paper

— predicts new transport, optical, and neutron-optical effects for ferromagnetic systems with a noncoplanar magnetization distribution;

— develops nanolithography and probe microscopy techniques that create vortex, antivortex, and spiral magnetization distributions in ferromagnetic nanostructures;

— establishes that, in multilayered ferromagnetic particles of anisotropic shape, stable collinear states of different resistance exist, making these systems promising for application in information storage and processing devices.

While there has been some success in the study of inhomogeneously magnetized ferromagnetic structures, thus far none of the predicted 'exchange' effects have been observed. Noting also that many relevant topics are left unaddressed in this paper [including those related to the magnetoelectric effect in inhomogeneous magnets [33, 34], to phenomena in nonstationary and inhomogeneous magnetic structures (see, for example, Ref. [35]), etc.], it is safely concluded that the topic is far from exhausted and further research remains to be done.

Acknowledgments. This work was supported by RFBR (grants 11-02-00294-a, 11-02-00589-a, and 11-02-00434-a), by the programs 'Fundamental Studies in Nanotechnologies and Nanomaterials', 'Spin Phenomena in Solid-State Nanostructures and Spintronics', and 'Quantum Macrophysics' of the Russian Academy of Sciences, and by the Russian Federation Ministry of Education and Science.

References

1. Baibich M N et al. *Phys. Rev. Lett.* **61** 2472 (1988)
2. Binasch G et al. *Phys. Rev. B* **39** 4828 (1989)
3. Julliere M *Phys. Lett. A* **54** 225 (1975)
4. Vonsovskii S V *Magnetizm* (Magnetism) (Moscow: Nauka, 1971) [Translated into English (New York: J. Wiley, 1974)]
5. Landau L D, Lifshitz E M *Elektrodinamika Sploshnykh Sred* (Electrodynamics of Continuous Media) (Moscow: Nauka, 1982) [Translated into English (Oxford: Pergamon, 1984)]
6. Andreev A F, Marchenko V I *Usp. Fiz. Nauk* **130** 39 (1980) [*Sov. Phys. Usp.* **23** 21 (1980)]
7. Fraerman A A, Udalov O G *Phys. Rev. B* **77** 094401 (2008)
8. Mironov V L et al. *Phys. Rev. B* **81** 094436 (2010)
9. Aharonov Ya, Stern A *Phys. Rev. Lett.* **69** 3593 (1992)
10. Izyumov Yu A, Naish V E, Ozerov R P *Neitronografiya Magnetikov* (Neutron Diffraction of Magnetic Materials) (Moscow: Atomizdat, 1981) [Translated into English (New York: Consultants Bureau, 1991)]
11. Matveev V M, Nagaev É L *Zh. Eksp. Teor. Fiz.* **69** 2151 (1975) [*Sov. Phys. JETP* **42** 1094 (1975)]
12. Loss D, Goldbart P, Balatsky A V *Phys. Rev. Lett.* **65** 1655 (1990)
13. Tatara G, Kohno H *Phys. Rev. B* **67** 113316 (2003)
14. Karashtin E A, Udalov O G, Fraerman A A *Zh. Eksp. Teor. Fiz.* **136** 1127 (2009) [*JETP* **109** 973 (2009)]
15. Fraerman A A, Udalov O G Pis'ma *Zh. Eksp. Teor. Fiz.* **87** 187 (2008) [*JETP Lett.* **87** 159 (2008)]
16. Karashtin E A, Udalov O G *Zh. Eksp. Teor. Fiz.* **140** 1134 (2011) [*JETP* **113** 992 (2011)]
17. Ignatovich V K, Nikitenko Yu V, Fraerman A A *Zh. Eksp. Teor. Fiz.* **137** 886 (2010) [*JETP* **110** 775 (2010)]
18. Tatarskii D A, Udalov O G , Fraerman A A *Zh. Eksp. Teor. Fiz.* **142** 710 (2012) [*JETP* **115** 626 (2012)]; arXiv:1101.2735
19. Cowburn R P et al. *Phys. Rev. Lett.* **83** 1042 (1999)
20. Mironov V L et al. *J. Appl. Phys.* **106** 053911 (2009)
21. Chang J et al. *J. Appl. Phys.* **100** 104304 (2006)
22. Mironov V L et al. *Fiz. Met. Metalloved.* **110** 708 (2010) [*Phys. Met. Metallogr.* **110** 708 (2010)]
23. Vdovichev S N et al. *Fiz. Tverd. Tela* **48** 179 (2006) [*Phys. Solid State* **48** 1902 (2006)]
24. Yakata S et al. *Appl. Phys. Lett.* **97** 222503 (2010)
25. Udalov O G et al., arXiv:1204.2461
26. Kosevich A M, Ivanov B A, Kovalev A S *Nelineinye Volny Namagnichennosti: Dinamicheskie i Topologicheskie Solitony* (Nonlinear Magnetization Waves: Dynamical and Topological Solitons) (Kiev: Naukova Dumka, 1983)
27. Kosevich A M, Ivanov B A, Kovalev A S *Phys. Rep.* **194** 117 (1990)
28. Neubauer A et al. *Phys. Rev. Lett.* **102** 186602 (2009)
29. Vdovichev S N et al. *Pis'ma Zh. Eksp. Teor. Fiz.* **94** 418 (2011) [*JETP Lett.* **94** 386 (2011)]
30. Fraerman A A et al. *J. Appl. Phys.* **103** 073916 (2008)
31. Mukhamatchin K R, Fraerman A A *Pis'ma Zh. Eksp. Teor. Fiz.* **93** 797 (2011) [*JETP Lett.* **93** 716 (2011)]
32. Slonczewski J C *Phys. Rev. B* **39** 6995 (1989)
33. Zvezdin A K, Pyatakov A P *Usp. Fiz. Nauk* **179** 897 (2009) [*Phys. Usp.* **52** 845 (2009)]
34. Zvezdin A K, Pyatakov A P *Usp. Fiz. Nauk* **182** 593 (2012) [*Phys. Usp.* **55** 557 (2012)]
35. Fraerman A A, Muhamatchin K R, Tokman I D *Phys. Rev. B* **84** 012402 (2011)

PACS numbers: **61.72.–y**, **62.20.–x**, **62.30.+d**
DOI: 10.3367/UFNe.0182.201212i.1351

Nonlinear wave processes in a deformable solid as in a multiscale hierarchically organized system

V E Panin, V E Egorushkin, A V Panin

1. Introduction

In this report, we theoretically and experimentally substantiate the conception of a multiscale description of a deformable solid as a nonlinear hierarchically organized system. The surface layers and all internal interfaces are considered as an independent planar functional subsystem with a short-range order. The channelled plastic flow in the planar subsystem is primary. It is responsible for the formation and emission of all types of strain-induced defects into the crystalline subsystem. This process is developed through the mechanism of nonlinear waves which determine the law of self-consistency of

V E Panin, V E Egorushkin, A V Panin Institute of Strength Physics and Materials Science, Siberian Branch of the Russian Academy of Sciences, Tomsk, Russian Federation
E-mail: paninve@ispms.tsc.ru

Uspekhi Fizicheskikh Nauk **182** (12) 1351 – 1357 (2012)
DOI: 10.3367/UFNr.0182.201212i.1351
Translated by S N Gorin; edited by A Radzig